VOLUME-6 | ISSUE-2 | FEBRUARY-2017 • ISSN No 2277 - 8179 | IF : 3.508 | IC Value : 78.46

Photocatalytic and Antibacterial Properties of ZnO:TiO_2 Nanocomposite

Physics

KEYWORDS: Nanocomposite, triple-exponential decay, diamagnetism, photocatalyitc degradation, microbial toxicity

Rajaram Rajakumari — PG and Research Department of Physics, Queen Mary's College, Chennai – 600 004, India.

Rita John — Department of Theoretical Physics, University of Madras, Chennai – 600 020, India

Mahalingam Umadevi — Department of Physics, Mother Teresa Women's University, Kodaikanal – 624101, India

ABSTRACT

The ZnO:TiO_2 nanocomposite of varying molar ratios were synthesized by wet chemical reaction method. The XRD studies exhibit the presence of wurtzite (hexagonal) crystal structure similar to the parent compound (ZnO) in 5 mol% TiO_2 doped ZnO, suggesting that doped Ti^{4+} ions sit at the regular Zn^{2+} sites. However, same studies spread over the samples with Ti^{4+} content > 5 mol% reveals the occurrence of additional peaks corresponding to TiO_2. Triple exponential decay was observed in the fluorescence life time measurement (FLIM) of the synthesized samples. The magnetic properties measured from VSM data revealed diamagnetism in ZnO: TiO_2 nanocomposites. The photocatalytic activity of ZnO: TiO_2 (20, 30, and 40 mol%) in the photocatalytic degradation of methyl orange showed enhanced degradation effect for 40 mol% ZnO: TiO_2. The antibacterial activity of the ZnO: TiO_2 was evaluated for three different bacteria by agar disc diffusion assay and the results clearly showed that ZnO: TiO_2 nanocomposite has remarkable antibacterial effect and this effect is concentration-dependent. While increasing the concentration of TiO_2, more microbial toxicity was observed.

I. Introduction

Doped ZnO has attracted much attention due to their unique and versatile properties of optical sensing [1], gas sensing [2] and piezoelectric sensing [3] for various applications. Being a wide band gap semiconductor, ZnO is also useful for other possible applications in the field of optoelectronic devices such as ultra – violet (UV) light emitting diodes (LEDs), blue luminescent devices, low threshold room temperature UV lasers, solar cells and photo catalysts [4-7]. On the other hand, the undoped ZnO exhibits n-type conductivity, due to the formation of more native donor-type defects. To overcome this disadvantage, many research have been carried out on how the photoelectrical properties of ZnO are influenced by doping with the group III elements selected as the dopant materials [8], such as Ga [9] and Sn [10]. Many studies have been conducted on the sintering of several ZnO systems doped with CdO [11], $Sb2O_3$ [12], $MnCO_3$ [13], and CuO [14]. Among the semiconductor oxides, Titanium dioxide (TiO_2), a native oxygen-deficient metal oxide, with a band gap of 3.2eV has been undoubtedly proved to be an economically moderate dopant and potential sensing material.

ZnO and TiO_2 are the most versatile semi-conductor oxides with applications spanning a wide range from cosmetics to waterir purification [15, 16]. Most of the applications rely on the generation of electron–hole pairs upon excitation with electromagnetic waves that have energies higher than their band gaps. ZnO and TiO_2 are also reported as good photocatalysts for the degradation of environmental contaminants [17, 18]. TiO_2 is the most widely used metal oxide for environmental applications, paints, electronic devices, gas sensors and solar cells. It is a well known semiconductor with excellent photocatalytic property that has been widely used in environmental pollutant elimination, antibacterial dopes, self-clean buildings, etc. Its unique antibacterial properties make the material a candidate for applications in medical devices and sanitary ware surfaces. It is expected that the composites of ZnO and TiO_2 would exhibit useful applications in photocatalysis and in antimicrobial study. In this work, we present a simple procedure for obtaining ZnO: TiO_2 nanocomposite by wet chemical route and their characterization as a first step to enhance the photocatalytic efficiency of the composite.

II. Experimental

To synthesize 5 mol % of TiO_2 doped ZnO, 6.132g of $ZnCl_2$ and 0.399g of TiO_2 were dissolved in 50 ml distilled water under magnetic stirring at a temperature of 100°C to form a transparent solution (Solution A). NaOH (4.399 g) was dissolved in 30 ml distilled water (solution B) and added dropwise into solution A while stirring until a milk-white solution was formed. This mixture was centrifuged at 1000 rpm for 30 min and then the precipitate was washed with distilled water and ethanol for several times and dried at 200°C for 2 hours in oven to obtain ZnO: TiO_2 nanopowder. In this manner the other molar ratios (10, 20, 30, and 40) of ZnO: TiO_2 were prepared.

III. Results and Discussion

(1) Structural Characterization

The XRD pattern of the synthesized ZnO:TiO_2 nanopowder of different concentrations is shown in Figure 1. The XRD pattern of 5 mol% TiO_2 doped ZnO showed a set of well defined diffraction peaks and this could be indexed to the wurtzite hexagonal phase of ZnO. Moreover, diffraction peaks corresponding to TiO_2 is also observed in the XRD patterns recorded from the other concentrations of ZnO: TiO_2 due to the formation of ZnO:TiO_2 nanocomposite. Intense and narrow peaks, observed in the XRD imply good crystalline nature of the synthesized nanoparticles. The average crystallite size of the synthesized samples, calculated using Scherer equation is found to increase with the increasing concentration of TiO_2 in ZnO (Table 1). The difference in band gap between the bulk and nano (ΔEg) decreased with the increasing concentration of TiO_2. The specific surface of ZnO:TiO_2 nanocomposite is found to decrease as the concentration increases due to increase in the crystallite size.

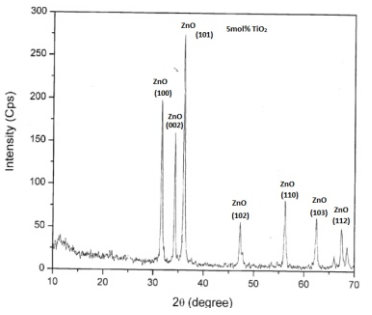

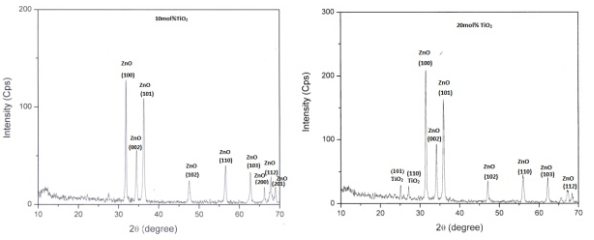

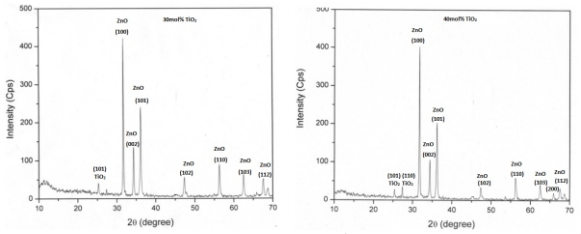

Figure 1 XRD patterns of ZnO:TiO_2 (5, 10, 20, 30 & 40 mol %) nanopowder

Table 1. Average crystallite size, Specific surface area and Difference in band gap of ZnO: TiO_2 Nanocomposite

Description	Average crystallite size (nm) $D=\frac{0.9\lambda}{\beta\cos\theta}$	Specific surface area (m^2/g) $S=\frac{6\times10^3}{D_p\rho}$	Difference in band gap $\Delta Eg = Eg^n - Eg^b = h^2/8a^2 (1/m_e + 1/m_h)$ (eV)
5 molar %	44	23.09	0.0012460
10 molar %	46	22.09	0.0011650
20 molar %	48	21.16	0.0010470
30 molar %	52	19.53	0.0008923
40 molar %	55	18.47	0.0007970

(2) Determination of dislocation density from XRD analysis

Dislocations play a key role in determining the mechanical properties of materials. The XRD peak profile analysis suggests that the dislocation densities for ZnO: TiO_2 (5, 10, 20, 30, and 40 mol %) vary slightly in the range (0.6 – 1.3) X1015 m-2 (Table 2) for (100), (002), and (101) orientations. In the concentration range of 5 mol% to 20 mol%, the dislocation density (δ) along three directions (100), (002) and (101) remains at 3.5 X1015 m-2. From 5 mol% to 10 mol% of TiO_2 in ZnO, the dislocation density shifts from (100) plane to (002) plane, where the concentration increases along (002) plane at the expense of that along (100) plane. The dislocation density (δ) along (101) plane remains almost the same. However, for concentrations 30 mol%, dislocation density (δ) along (100), (002) and (101) has reduced. This is attributed to the increase in the crystallite size which could have accommodated the atoms with reduced dislocations.

Table 2 Dislocation Density of ZnO: TiO_2 in the (100), (002) and (101) planes

Sample	Dislocation Density $\delta = 15\beta\cos\theta / 4aD$ (m-2)			Total Dislocation density (m-2)
	(1 0 0)	(0 0 2)	(1 0 1)	
5 molar %	$1.3452X10^{15}$	$0.6378X10^{15}$	$1.4930X10^{15}$	$3.476\ X10^{15}$
10 molar %	$0.6010\ X10^{15}$	$1.4411\ X10^{15}$	$1.4990\ X10^{15}$	$3.541\ X10^{15}$
20 molar %	$1.3399\ X10^{15}$	$0.6359\ X10^{15}$	$1.4880\ X10^{15}$	$3.464\ X10^{15}$
30 molar %	$0.5185\ X10^{15}$	$0.6386\ X10^{15}$	$0.1496\ X10^{15}$	$1.307\ X10^{15}$
40 molar %	$0.5997\ X10^{15}$	$0.6399\ X10^{15}$	$0.6657\ X10^{15}$	$1.905\ X10^{15}$

***(3)* XRD – Williamson Hall Plot**

Williamson and Hall proposed a method for deconvoluting size and strain broadening by looking at the peak width as a function of 2θ. W-H plot is a classical method to obtain qualitative information of anisotropy in broadening. Williamson and Hall [19] assumed that both size and strain broadened profiles are Lorentzian. If the points in the W - H plot are scattered, the broadening is termed as anisotropic. Figure 2 shows the W-H plot for ZnO: TiO_2 for 5, 10, 20, 30, and 40 mol% concentrations. It is observed from the figure that the line broadening is not a monotonous function of the diffraction angle indicating the anisotropic broadening of the line profile in all the cases. The strain value extracted from the linear fit of W-H plot ranges from 0.001 to 0.003, and crystallite size vary from 35 to 58 nm.

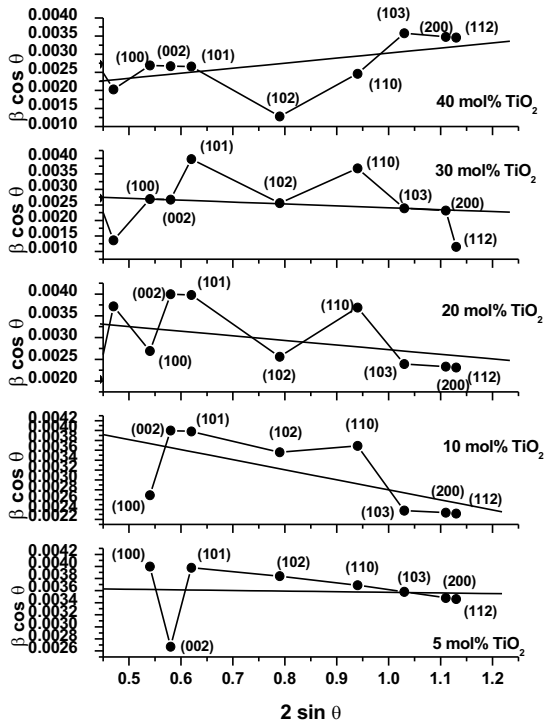

Figure 2 W-H Plot of ZnO: TiO_2

***(4)* Morphological Study of ZnO: TiO_2**

The surface morphology of ZnO: TiO_2 was studied by SEM. The SEM images shown in Figure 3 were recorded for 5 mol% TiO_2 doped ZnO. The SEM micrographs show the polycrystalline nature of the TiO_2 doped nano ZnO. It is also observed from the SEM images that the nanoparticles are uniformly stacked, and agglomerated. This may be attributed to the fact that ZnO nanoparticles have the tendency to agglomerate due to their high surface energy and high surface tension of the ultrafine nanoparticles. The average particle size observed from SEM images is 60 nm. The fine particle size results in a large surface area that in turn enhances the catalytic activity of the nanoparticles.

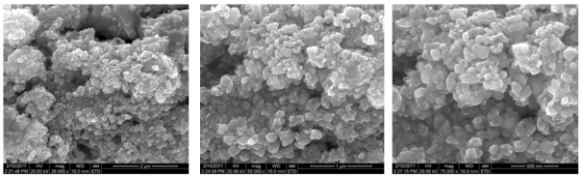

Figure 3 SEM images of 5 mol% ZnO: TiO_2 nanocomposite powder

***(5)* UV absorption study of ZnO: TiO_2**

Figure 4 shows the UV absorption band edge emission of ZnO: TiO_2 nanocomposites. It is observed that for 5 mol% TiO_2 doped ZnO, the band gap increases from 3.37 eV (bulk ZnO) to 3.45 eV. The energy band gap measured from the absorption spectra of TiO_2 doped ZnO (10 mol%, 20 mol%, and 30 mol %) is found to decrease to a value of 3.15 eV. As the concentration TiO_2 in ZnO increases, the band gap is found to be decreasing which is also accompanied with the increase in the size of the nanoparticles. This is due to the increase in the metallicity on doping with TiO_2. Thus, a decrease in covalency and an increase in the ionicity are observed in the iono-covalent ZnO due to doping. It is also observed from the figure that, a strong UV absorption band for TiO_2 doped ZnO nanoparticles. It is assigned to the ZnO band-to-band transition and the intra d-d transition of Ti^{4+} ions in the ligand field from ZnO wurtzite structure. The appearance of intra d-d transition indicates that the Ti^{4+} ions are doped in Zn sites

VOLUME-6 | ISSUE-2 | FEBRUARY-2017 • ISSN No 2277 - 8179 | IF : 3.508 | IC Value : 78.46

successfully.

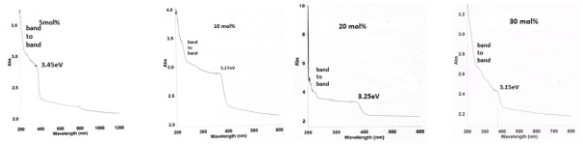

Figure 4 UV absorption spectra of ZnO: TiO_2 nanocomposites

***(6)* Photoluminescence (PL) study of ZnO: TiO_2**

The PL spectra of ZnO: TiO_2 nanocomposites (Figure 5) showed the PL characteristics with the peaks in visible region (Blue, Green) and UV region between 2.94 to 2.35 and 3.2 to 3.55 eV respectively, after laser excitation with wavelength 370 nm, 284 nm, and 255 nm. The UV emission peak with 3.20 eV (for 20 mol%) and 3.55eV (for 40 mol%) may be due to the excitonic recombination through single optical phonon or two phonon process near the band edge levels of ZnO with increasing TiO_2 mole fraction, and those excitonic peaks became more prominent. The visible emission peaks observed at 2.94 eV (for 5 mol %) and 2.35 eV (for 30 mol%) were due to donor-acceptor pair recombination involving different defect levels in the nanocrystals.

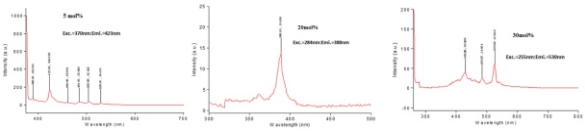

Figure 5 PL spectra of ZnO:TiO_2 nanocomposites

***(7)* Florescence life time measurement (τ_F) of ZnO: TiO_2**

Fluorescence or phosphorescence lifetime measurements are often used to investigate the various modes of de-excitation that occur following photo-excitation. The fluorescence life time measurement studies of ZnO:TiO_2 (Figure 6, Table 3) show a triple-exponential decay. This is due to non-homogeneity in size and shape of the nanoparticles. The life time (τ_3) with maximum amplitude decreases from 84.48 nano second (ns) to 79.38 ns as the concentration of TiO_2 increased from 5 mol% to 20 mol% (Table 3). This value increased to 117.26 ns for 30 mol%, and decreased again to 97.16 ns for 40 mol%. Hence it is concluded that the fluorescence nature of ZnO was not affected due to the dopant, TiO_2 even at higher level concentration.

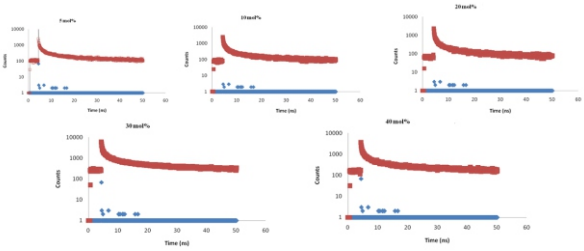

Figure 6 Triple exponential florescence decay curves of ZnO : TiO_2 nanocomposites

Table 3 Fluorescence decay parameters of ZnO: TiO_2

Sample	$\lambda_{exc.}$ (nm)	λ_F (nm)	τ_F (ns)	B	χ^2
5 molar %	380	420	τ_1 = 2.32 τ_2 = 13.89 τ_3 = 84.48	B_1=0.16 B_2=0.075 B_3=0.036	0.9722
10 molar %	380	380	τ_1 = 1.07 τ_2 =11.15 τ_3 =81.80	B_1=0.11 B_2=0.097 B_3=0.037	1.0625
20 molar %	380	530	τ_1 = 1.55 τ_2 = 10.70 τ_3 = 79.38	B_1=0.317 B_2=0.097 B_3=0.032	1.0379
30 molar %	380	350	τ_1 = 3.00 τ_2 =18.92 τ_3 =117.26	B_1=0.56 B_2=0.17 B_3=0.087	1.1328
40 molar %	380	430	τ_1 = 2.50 τ_2 = 14.29 τ^3 = 97.16	B_1=0.216 B_2=0.114 B_3=0.055	1.2343

***(8)* Confocal Laser Scanning Microscopy Images (CLSM) of ZnO: TiO_2**

The technique of laser scanning and spinning disk Confocal fluorescence microscopy has become an essential tool in biology and the biomedical sciences, as well as in materials science due to attributes that are not readily available using other contrast modes with traditional optical microscopy. The CLSM images of ZnO: TiO_2 (Figure 7) exhibited green emission when the samples were excited with laser beam of wavelength 380 nm. This could be an indication that these materials have fluorescent nature. Hence these materials can be used as a suitable candidate for Fluorescence resonance Energy Transfer (FRET) applications.

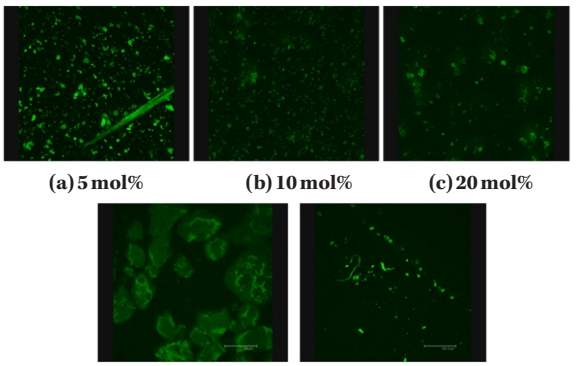

(a) 5 mol% **(b) 10 mol%** **(c) 20 mol%**

(d) 30 mol% **(e) 40 mol%**

Figure 7 Confocal Laser Scanning Images of ZnO: TiO_2

(9) VSM measurement of ZnO: TiO_2

Transition metal (TM) doped ZnO has garnered special interest as diluted magnetic semiconductor material (DMS) due to their potential application in spintronics. Magnetic and magnetic semiconducting nanoparticle systems have interesting properties due to surface and finite size effects which are different from the bulk properties. The presence of TM ions in DMS leads to an exchange interaction between itinerant sp- band electrons or holes and the d-electron spins localized at the magnetic ions, resulting in versatile magnetic-field-induced functionalities.

The hysteresis loop of the material is the best representation of all its magnetic properties. The magnetic moment versus field (M–H) curves of 5 and 10 mol% ZnO:TiO_2 are shown in Figure 8. It is observed that the sample has no magnetization at zero field. When the field is applied, a small negative moment is induced which is proportional to the applied field strength. As the field is reduced the induced moment is reduced. This reveals the diamagnetic nature of the sample with negative slope of the hysteresis curve with negative susceptibility.

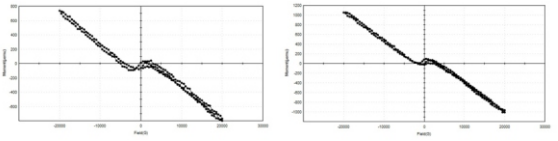

5 mol% **10 mol%**

Figure 8 M-H curves of ZnO: TiO_2

***(10)* Photocatalytic studies of ZnO: TiO_2 Nanocomposite**

The photocatalytic activity of three different concentrations (20, 30 and 40 mol%) of ZnO:TiO_2 nanocomposite was studied in the photocatalytic degradation of Methyl Orange (MO) in aqueous solution under UV irradiation (365 nm). Experiments were performed at different UV irradiation time. Figure 9 shows the optical absorption spectra of MO with three concentrations of ZnO: TiO_2 at

different irradiation time. The optical absorption spectra shows that the intensity of the absorption is decreasing gradually as the time increases, indicates that MO is suffering degradation during the photocatalytic reaction under UV irradiation [19]. The photocatalytic degradation of MO with reaction time is a first order as confirmed by the linear transforms of ln(Ct/Co) ~ t shown in Figure 10, from which the apparent rate constants can be obtained [20]. The Kapp value of ZnO: TiO_2 (20, 30 and 40 mol %), were 0.139, 0.188, and 0.196 min_1 respectively. In both cases, ZnO: TiO_2 (20 mol %) shows low decomposition rate compared with ZnO: TiO_2TiO_2 (30 and 40 mol %). It can be seen that the degradation rate of ZnO: TiO_2 (40 mol %) is very higher than ZnO: TiO_2 (20 and 30 mol %), and its photocatalytic activity has increased. Accordingly, more photo-induced electron and holes can be produced resulting in more superoxy species to participate photocatalytic degradation reaction. Thus, it is concluded from this study that the ZnO: TiO_2 (40 mol %) showed enhanced photocatalytic activity in comparison with the other concentrations of ZnO: TiO_2 (20 and 30 mol %).

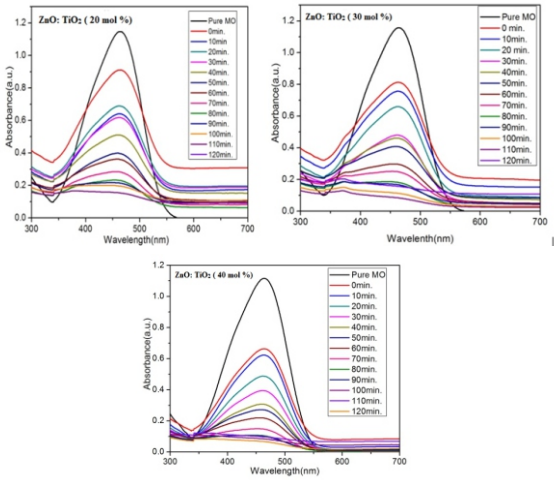

Figure 9 Optical absorption spectra of MO with ZnO: TiO_2 (20, 30 and 40 mol %) in different irradiation time

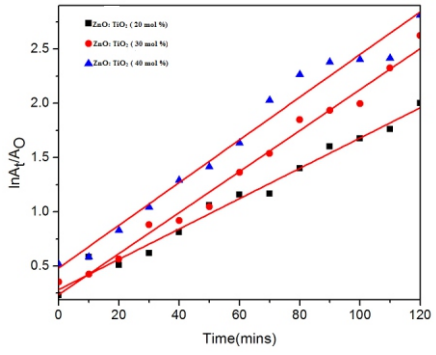

Figure 10 Rate of decomposition of MO in ZnO: TiO_2 (20, 30, and 40 mol %,) against Irradiation time

***(11)* Antibacterial study:**

Earlier studies have demonstrated that ZnO nanoparticles have antibacterial activity on both gram positive and negative bacteria including E.coli and also reported that the antibacterial activity of ZnO is dependent on the size and concentration of the ZnO nanoparticles. In the present study, our interest was to determine if ZnO: TiO_2 nanocomposites of different concentrations (20, 30 and 40 mol %) could be employed to inhibit the growth or kill various bacterial strains.

The bacteriological tests were conducted with *Staphylococcusaureus, E. coli* and *Bacillus subtilis* by agar diffusion method [21]. It is observed that the zone of inhibition increases as the concentration of TiO_2 in ZnO increases (Figure 11).

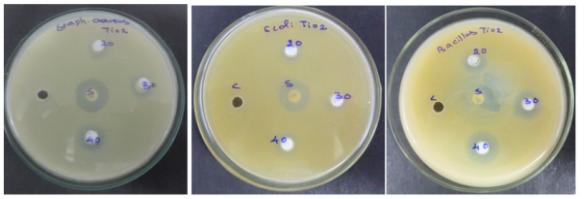

Figure 11 Antibacterial activity of ZnO:TiO_2 nanocomposites against tested bacteria by a disc diffusion method

VI. Conclusion

The ZnO: TiO_2 nanocomposites were successfully synthesized via wet chemical reaction method at low cost. These nanoparticles can be well indexed to the single phase of wurtzite ZnO with additional peaks corresponding to TiO_2 occurred, when the ZnO: TiO_2 ratio was more than 5 mol%. The average crystallite size calculated using Scherer equation increased as the dopant concentration increased. W-H plot generated for all the concentrations of TiO_2 doped ZnO nanoparticles showed that the broadening is highly anisotropic. The PL spectra of TiO_2 doped ZnO nanoparticles of all the concentrations indicated distinct excitonic and defect related peaks with systematic intensity variation with variation of TiO_2 doping percentage in ZnO. The PL spectra also revealed the visible emission from ZnO: TiO_2 nanocomposites, which have been supported by CLSM images of the same. The fluorescence decay profiles of TiO_2 doped ZnO were best fitted by a tri-exponential expression. The VSM measurements at room temperature indicated the diamagnetic nature of the sample with negative susceptibility. In the photocatalytic study, the 40 mol % ZnO: TiO_2 had a higher activity under UV light irradiations than the other concentrations. The antibacterial study showed that ZnO: TiO_2 nanocomposite had remarkable antibacterial effect.

Acknowledgements

This work was supported by Minor Research Project (sanctioned to R.R.) from University Grants Commission, New Delhi.

References

1. Özgür, Ü., Alivov, Ya.I., Liu, C., Teke,C., Reshchikov, M.A., Doğan, S., Avrutin, V., Cho, S.-J., Morkoç, H.: A comprehensive review of ZnO materials and devices, J. Appl. Phys., 89, [4], 041301-041403, (2005).
2. Maity, A.B., Chaudhuri S.: Gas Sensing Properties of ZnO Nanowires, Trans. Ind. Ceram. Soc., 67, [1], 1-15, (2008).
3. Liu, C.: Foundations of MEMS, (2nd Edn), Pearson Education, Inc., New York, (2012)
4. Kang, H.S., Kang, J.S., Kim, J.W., Lee, S.Y.: Annealing effect on the property of ultraviolet and green emissions of ZnO thin films, J. Appl. Phys., 95, [3], 1246-1250, (2004).
5. Gong, H., Hu, J.Q., Wang, J.H., Ong, C.H., Zhu, F.R.: Nano-crystalline Cudoped ZnO thin film gas sensor for CO, Sens. Actuator. B: Chemical, 115, [1], 247-251, (2006).
6. Aoki, T., Hatanaka, Y., Look, D.C.: ZnO diode fabricated by excimer-laser doping, Appl. Phys. Lett. 76, [22] 3257-32358, (2000).
7. Song, D., Aberle, A.G., Xia, J.: Optimisation of ZnO:Al films by change of sputter gas pressure for solar cell application, Appl. Surf. Sci., 195, [1–4], 291–296, (2002).
8. Janisch, R., Gopal, P., Spaldin, N.A.: Transition metal-doped TiO_2 and ZnO-present status of the field, J. Phys. Cond. Matt., 17, [27], R657-R690.
9. Moon, Y-K., Kim, S-H, Moon, D-Y., Kim, W-S., Park, J-W.: Enhancement of the electrical properties of GZO thin films on polycarbonate substrates by using a TiO2 buffer layer, J. Korean Phys. Soc. 51, [5], 1732-1735, (2007).
10. Ali, I., Ullah, Z., Siraj, K. Rafique, M.S., Khaleeq-ur-Rahman, M.: Sn doped ZnO thin films prepared by pulsed laser deposition for photovoltaic applications. Int. J. Thin Film Sci. Tec. 3, [3], 107-111 (2014).
11. Bodade, A.B., Bende, A.M, Chaudhari, G.N.: Synthesis and characterization of CdO-doped nanocrystalline ZnO: TiO2-based H2S gas sensor, Vacuum. 82, [6], 588-593, (2008).
12. Bernik, S., Daneu, N., Rečnik, A.: Inversion boundary induced grain growth in TiO2 or Sb2O3 doped ZnO-based varistor ceramics, J. Eur. Ceram. Soc., 24. [15-16], 3703-3708, (2004).
13. Wang, G., Wu, S., Su, H.: Microwave dielectric ceramics in the BaO–TiO_2–ZnO system doped with MnCO3 and SnO2, Mater. Lett., 59, [17], 2229–2231, (2005).
14. CorpuzI, R.D., Albia, J.R.: Electrophoretic fabrication of ZnO/ZnO-CuO composite for ammonia gas sensing, Mat. Res., 17, [4], 851-856, (2014).
15. Chekirab, N., Benhabilesa, O., Tassalitab, D., Laoufib, N.A., Bentaharb, F.: Photocatalytic degradation of methylene blue in aqueous suspensions using TiO_2 and ZnO, Desalinat. Water Treat. A, 57, [13], 6141-6147 (2016).
16. Wanga, J., Xiaa, Y., Dongb, Y., Chena R., Xianga, L., Komarnenib, S.: Defect-rich ZnO nanosheets of high surface area as an efficient visible-light photocatalyst, Appl. Cataly.B: Environ., 92, [5], 8-16, (2016).
17. Shaogui, Y., Xie, Q., Xinyong, L., Yazi, L., Shuo, C., Guohua C.: Preparation, characterization and photoelectrocatalytic properties of nanocrystalline Fe2O3/TiO_2, ZnO/TiO_2, and Fe2O_3/ZnO/TiO_2 composite film electrodes towards pentachlorophenol degradation, Phys. Chem. Chem. Phys., 6, [3], 659-664, (2004).
18. Yu, J., Wang, B.: Effect of calcination temperature on morphology and photoelectrochemical properties of anodized titanium dioxide nanotube array, Appl. Catal., B, 94, 295-302, (2010).

VOLUME-6 | ISSUE-2 | FEBRUARY-2017 • ISSN No 2277 - 8179 | IF : 3.508 | IC Value : 78.46

19. Umadevi, M., Parimaladevi, R., Sangari M.: Synthesis characterization and photocatalytic activity of fluorine doped TiO_2 nanoflakes synthesized using solid state reaction method, Spectrochim. Acta Part A: Mol. Biomol. Spectroscop. 120, 365–369, (2014).
20. Umadevi, M., Sangari, M., Parimaladevi, R., Sivanantham, A., Mayandi, J.: Enhanced photocatalytic, antimicrobial activity and photovoltaic characteristics of fluorine doped TiO_2 synthesized under ultrasound irradiation, J. Fluorine Chem. 156, 209–213, (2013).
21. Nagarajan, P., Rajagopalan, V.: Enhanced bioactivity of ZnO nanoparticles—an antimicrobial study, Sci. Technol. Adv. Mat., 9, [3], 1-7, (2008).